

Effect of nanoparticulate bioactive glass particles on bioactivity and cytocompatibility of poly(3-hydroxybutyrate) composites

Superb K. Misra^{1,2}, Tahera Ansari³, Dirk Mohn⁴,
Sabeel P. Valappil⁵, Tobias J. Brunner⁴, Wendelin J. Stark⁴,
Ipsita Roy⁶, Jonathan C. Knowles⁷, Paul D. Sibbons³,
Eugenia Valsami Jones², Aldo R. Boccaccini^{1,*} and Vehid Salih^{7,*}

¹*Department of Materials, Imperial College London, London SW7 2BP, UK*

²*Department of Mineralogy, Natural History Museum, Cromwell Road, London SW7 5BD, UK*

³*Department of Surgical Research, Northwick Park Institute for Medical Research, Northwick Park Hospital, Watford Road, Harrow HA1 3UJ, UK*

⁴*Department of Chemistry and Applied Biosciences, Institute for Chemical and Bioengineering, ETH Zurich, 8093 Zurich, Switzerland*

⁵*School of Dental Sciences, University of Liverpool, Liverpool L69 3GN, UK*

⁶*Department of Molecular and Applied Biosciences, University of Westminster, London W1W 6UW, UK*

⁷*Division of Biomaterials and Tissue Engineering, UCL Eastman Dental Institute, London WC1X 8LD, UK*

This work investigated the effect of adding nanoparticulate (29 nm) bioactive glass particles on the bioactivity, degradation and *in vitro* cytocompatibility of poly(3-hydroxybutyrate) (P(3HB)) composites/nano-sized bioactive glass (n-BG). Two different concentrations (10 and 20 wt %) of nanoscale bioactive glass particles of 45S5 Bioglass composition were used to prepare composite films. Several techniques (Raman spectroscopy, scanning electron microscopy, atomic force microscopy, energy dispersive X-ray) were used to monitor their surface and bioactivity over a 45-day period of immersion in simulated body fluid (SBF). All results suggested the P(3HB)/n-BG composites to be highly bioactive, confirmed by the formation of hydroxyapatite on material surfaces upon immersion in SBF. The weight loss and water uptake were found to increase on increasing bioactive glass content. Cytocompatibility study (cell proliferation, cell attachment, alkaline phosphatase activity and osteocalcin production) using human MG-63 osteoblast-like cells in osteogenic and non-osteogenic medium showed that the composite substrates are suitable for cell attachment, proliferation and differentiation.

Keywords: poly(3-hydroxybutyrate); composites; nanoparticles; bioactive glass; MG-63 human osteoblasts; tissue engineering

1. INTRODUCTION

The use of polymer/bioceramic composite systems in biomedical applications, including tissue engineering scaffolds has seen increasing impetus owing to the ability to tailor the properties (*viz.* mechanical strength, stiffness, degradation kinetics and biological response) by microstructural design (Rezwan *et al.* 2006; Guarino *et al.* 2007). One of the prime reasons for the use of a bioceramic phase is to induce the formation of a

bioactive hydroxyapatite (HA) layer on the surface that effectively interacts with the surrounding bone tissue (Hench 1998; Misra *et al.* 2006; Rezwan *et al.* 2006; Guarino *et al.* 2007; Barrere *et al.* 2008) and effectively also mimics the natural structure of bone (crucial for hard tissue applications; Barrere *et al.* 2008). Formation of the HA layer (Hench 1998) is a dynamic process and the kinetics of HA formation changes with time. Therefore, it is crucial to monitor the bioactivity of a biomaterial by using more than one means of characterization. The addition of bioactive ceramics or glasses to a biopolymer has also been shown to alter the degradation rate of the material by changing relevant parameters such as hydrophobicity, water

*Authors for correspondence (a.boccaccini@imperial.ac.uk; sfaavs@ucl.ac.uk).

Electronic supplementary material is available at <http://dx.doi.org/10.1098/rsif.2009.0255> or via <http://rsif.royalsocietypublishing.org>.

absorption, weight loss and pH (Li & Chang 2005b; Loher *et al.* 2006). Lately, the use of nano-sized bioactive glass (n-BG) particles in polymeric matrices has shown to enhance the mechanical properties of the composites (Liu *et al.* 2008; Misra *et al.* 2008), increase surface adsorption of proteins (Misra *et al.* 2008) and is being employed in injectable systems (Couto *et al.* 2009). Bioactive glass nanoparticles have also shown increased bactericidal effect compared with the conventional micron-sized bioactive glass particles (Waltimo *et al.* 2007). Obviously, evaluation of the biocompatibility of composite systems using *in vitro* cell culture models and *in vivo* studies is required to determine the efficacy of the developed composites for the final use in the target area of application (Chen & Wu 2005; Schneider *et al.* 2008).

Poly(3-hydroxybutyrate) (P(3HB)) belongs to the biodegradable polyhydroxyalkanoate family and has been used for a range of biomedical applications (Williams & Martin 2002; Chen & Wu 2005; Misra *et al.* 2006). A recent study conducted on the derivatives of P(3HB) showed that the end products from degradation of P(3HB) are not harmful to mouse glial cells (Xiao *et al.* 2007), which highlights the biocompatibility of the polymer. Various *in vivo* experiments have shown P(3HB)/HA composites to allow bone apposition and attachment of both hard and soft tissue onto its surface (Knowles & Hastings 1992; Luklinska & Bonfield 1997). In general, it is important to understand/demonstrate the presence of an optimum concentration of particulate bioceramic phase in a polymer, which affects the material degradation behaviour and surface bioactivity as well as enhances the osteoblast cell functional response (Blaker *et al.* 2003; Wang *et al.* 2005; Rezwan *et al.* 2006; Guarino *et al.* 2007).

In this study, we have examined, in detail, the bioactivity (with particular emphasis towards evaluating the build up of the biologically active HA layer), degradation behaviour and biocompatibility of substrates fabricated by combining P(3HB) and bioactive glass nanoparticles (45S5 type). The proliferation of MG-63 human osteoblasts on the composites was evaluated along with measuring the alkaline phosphatase (ALP) activity and osteocalcin production in osteogenic and non-osteogenic media. This research was conducted to enable a better assessment of the potential of the P(3HB)/n-BG composite for applications in bone tissue engineering (Blaker *et al.* 2003; Helen & Gough 2006).

2. EXPERIMENTAL METHODS

2.1. Sample preparation

P(3HB), $M_w = 285\,000$ was produced following previously developed biotechnological methods (Valappil *et al.* 2007) from *Bacillus cereus* SPV using a 20 l fermentor vessel. n-BG powders of nominal composition equivalent to 45S5 Bioglass (46 wt % SiO₂, 23 wt % Na₂O, 27 wt % CaO, 4 wt % P₂O₅), with spherical shape and a mean particle size of 29 nm, were prepared using the flame spray synthesis process, as described elsewhere (Brunner *et al.* 2006). P(3HB) and P(3HB)/

bioactive glass films (10 and 20 wt % n-BG) were prepared by solvent casting technique. Chloroform was used to dissolve P(3HB) using a polymer concentration of 3 wt %. Subsequently, n-BG particles were added to the polymer solution and sonicated for 1 min using a sonicating probe (Ultrasonic Homogenizers US200, Philip Harris Scientific, Leicestershire, UK) in order to break possible bioactive glass agglomerates and ensure a better (homogeneous) distribution of n-BG particles in the composite. The solution was then cast onto glass Petri dishes at room temperature. Films of nominally 0.12–0.14 mm thickness were produced. Once the films were cast, they were stored in desiccators for further analyses, as detailed below.

2.2. Simulated body fluid study of poly(3-hydroxybutyrate)/nano-sized bioactive glass composites

The *in vitro* bioactivity and degradation study for up to 45 days was carried out in simulated body fluid (SBF), as developed by Kokubo *et al.* (1990). The initial mass of the samples was recorded and specimens were immersed in SBF at 37°C. The approximate sample weight to SBF volume ratio was maintained as 0.07 g 50 ml⁻¹. The SBF was exchanged every 5 days and at different time points samples were collected for subsequent analyses.

2.3. Characterization techniques

Scanning electron microscopy. The samples before and after immersion in SBF were examined using a JEOL 5610LV scanning electron microscope. Energy dispersive X-ray (EDX) analysis was carried out on carbon coated samples at 15 kV and a working distance of 14 mm, using INCA (Oxford Instruments) software.

Atomic force microscopy. Atomic force microscopy (AFM) analysis was conducted on the polymeric and composite samples, using an Asylum MFP-3D-SA (Santa Barbara, USA) instrument in AC mode. The film samples (1 cm²) were placed on glass slides and were scanned in air over a 10 × 10 μm² area using an Olympus AC240TS tip (spring constant 2 N m⁻¹). The roughness of the surface as well as the amplitude and height channels were monitored and analysed using IGOR PRO software.

Water uptake and weight loss measurements. The water absorption (%WA) and weight loss (%WL) behaviour of samples, upon immersion in SBF, were determined over the 45-day period using equation (2.1), respectively,

$$\% \text{ WA} = \left(\frac{M_{t,\text{wet}} - M_{t,\text{dry}}}{M_{t,\text{dry}}} \right) \times 100 \quad (2.1)$$

$$\text{and} \quad \% \text{ WL} = \left(\frac{M_{0,\text{wet}} - M_{t,\text{dry}}}{M_{0,\text{dry}}} \right) \times 100,$$

where $M_{0,\text{dry}}$ is the original sample weight measured before immersion in SBF. For measuring the water absorption (%WA), immersed samples were removed at given time points, the surface gently wiped and the

weight was measured ($M_{t,wet}$). Similarly, for measuring the weight loss (%WL), the samples were removed from the SBF, dried at 37°C overnight and subsequently weighed ($M_{t,dry}$).

X-ray diffraction. X-ray diffraction (XRD) analysis on samples was performed on a Bruker D8 Advance diffractometer, in flat plate geometry, using Ni-filtered Cu K α radiation. Data were collected from 10° to 100° in θ - θ mode with a primary beam slit size of 0.6 mm. A Bruker Lynx Eye silicon strip detector was used and a step size of 0.02° and a count time of 0.1 s per step were employed.

Raman spectroscopy. All Raman spectra were recorded using a Raman spectrometer (LabRAM HR; Horiba Jobin Yvon Ltd, UK, with LABSPEC software) with a 633 nm laser, filter at 100 per cent, hole at 300, slit at 150, grating at 1800, microscope objective $\times 50$ and acquisition properties of exposure time for 10 s. Three spectra per location were recorded in the wavenumber interval of 400–1400 cm^{-1} .

2.4. Cytocompatibility studies

In vitro cell culture studies were performed using MG-63 human osteosarcoma cell line. MG-63 cells, obtained from ECACC (European Collection of Cell Cultures at the Health Protection Agency, UK) were cultured in growth medium (Dulbecco's modified Eagle's medium (DMEM); PAA, Germany), supplemented with 10 per cent (v/v) foetal calf serum, 1 per cent (v/v) penicillin and streptomycin solution and incubated at 37°C in a humidified atmosphere (5% CO₂ in 95% air), with the medium changed every 2 days.

The samples (1 cm^2) were UV sterilized for 30 min and passivated in DMEM culture medium for 12 h, prior to seeding the cells. As a result of this passivation treatment, the presence of nitrogen and a gradual increase of calcium and phosphate precipitation on the samples was expected (Faure *et al.* 2009). A seeding density of 20 000 cells cm^{-2} was used, and the specified amounts of cells were seeded using 1 ml of DMEM medium. The plates were incubated in a humidified environment for a period of up to 14 days and the medium was changed every second day. At specific time intervals, samples were analysed for cell proliferation, ALP activity and osteocalcin measurements. Analyses were carried out in triplicates, per sample, and standard tissue culture plastic was used as the control.

Cell proliferation study. The cell proliferation study ($n = 3$) was carried out using the Alamar blue (AB) assay. AB (AbD Serotec, UK) was added to the samples (10% v/v of medium) and incubated at 37°C for 4 h. Aliquots of 200 μl from each sample well were transferred to a black 96-well plate and the fluorescence of the samples was measured using a fluorescence plate reader (Fluoroskan, Lab Systems) at 560 nm (A_{560}) and 590 nm (A_{590}). AB is an indicator dye that incorporates an oxidation–reduction (REDOX) indicator that both fluoresces and changes colour in response to the chemical reduction in growth medium, resulting from cell growth. The AB assay is designed to quantitatively measure the proliferation of various human and animal cell lines. AB is preferred to other cell

proliferation/growth assays such as 3-(4,5-dimethylthiazolyl-2)-2,5-diphenyltetrazolium bromide (MTT) because it measures proliferation in the same population of cells in real time, whereas MTT requires separate replicates to be used for each time point. AB is non-toxic and does not interfere with viability, as is the case with the use of Trypan Blue, for example.

Alkaline phosphatase activity. Basal levels of cellular ALP activity of the MG-63 cells grown on the P(3HB)/n-BG composites were measured after 1, 7 and 14 days. The ALP study was conducted on two batches of samples, one batch in which the cell medium was non-osteogenic (used for the cell proliferation study) and the other batch containing osteogenic medium (i.e. non-osteogenic medium + 50 $\mu\text{g ml}^{-1}$ of vitamin C + 10 mM of β -glycerophosphate). ALP was measured using a commercially available SensoLyte p-Nitrophenol phosphate (pNPP) Alkaline Phosphatase Assay kit (AnaSpec, USA). The kit acts as a colorimetric assay for detecting ALP with a phosphatase conjugated secondary antibody by using pNPP as a phosphatase substrate. Samples ($n = 3$) were prepared as per the manufacturer's protocol and ALP standard was prepared in a serial dilution of 1 : 50 and detected using an absorbance of 405 nm.

Osteocalcin measurements. Osteocalcin production of the cells grown on the substrates incubated in osteogenic and non-osteogenic medium was measured ($n = 3$) at 1, 7 and 14 days using a commercially available Gla-type osteocalcin EIA kit (TaKaRa Bio Inc., Japan). The GLA-type osteocalcin kit is an *in vitro* enzyme immunoassay kit for quantitative determination of human carboxylated type of osteocalcin (Gla-OC) in medium. The standard curve was obtained by preparing serial dilutions and reading the absorbance at 450 nm.

Specimen preparation for SEM. Polymeric and composite films were examined under SEM to observe MG-63 cell spreading and attachment on the surface of the samples. Day 4 and 7 specimens were fixed in 3 per cent glutaraldehyde in 0.1 M cacodylate buffer for 12 h at 4°C. Subsequent dehydration using a series of graded ethyl alcohols (50%, 70%, 90% and 100%) was performed. Samples were then critically point dried by immersion in hexamethyldisilazane for 2 min and left in a fume cupboard for 2 h for subsequent drying. The dried samples were then attached to aluminium stubs, gold coated and examined under SEM (JEOL 5610LV, JEOL, USA) at an acceleration voltage of 10–15 kV.

Statistical analysis. All data are expressed as mean \pm s.d. The data were compared using Student's *t*-test and differences were considered significant when $*p < 0.05$, $**p < 0.01$ and $***p < 0.001$. $p > 0.05$ was taken as indicating no significant difference.

3. RESULTS

3.1. Microstructural analysis

The addition of n-BG particles is seen to change the surface morphology considerably compared with the P(3HB) samples by inducing a rough topography, as qualitatively examined by SEM (figure 1*a–c*). It is noted that the exposure of n-BG particles on the surface

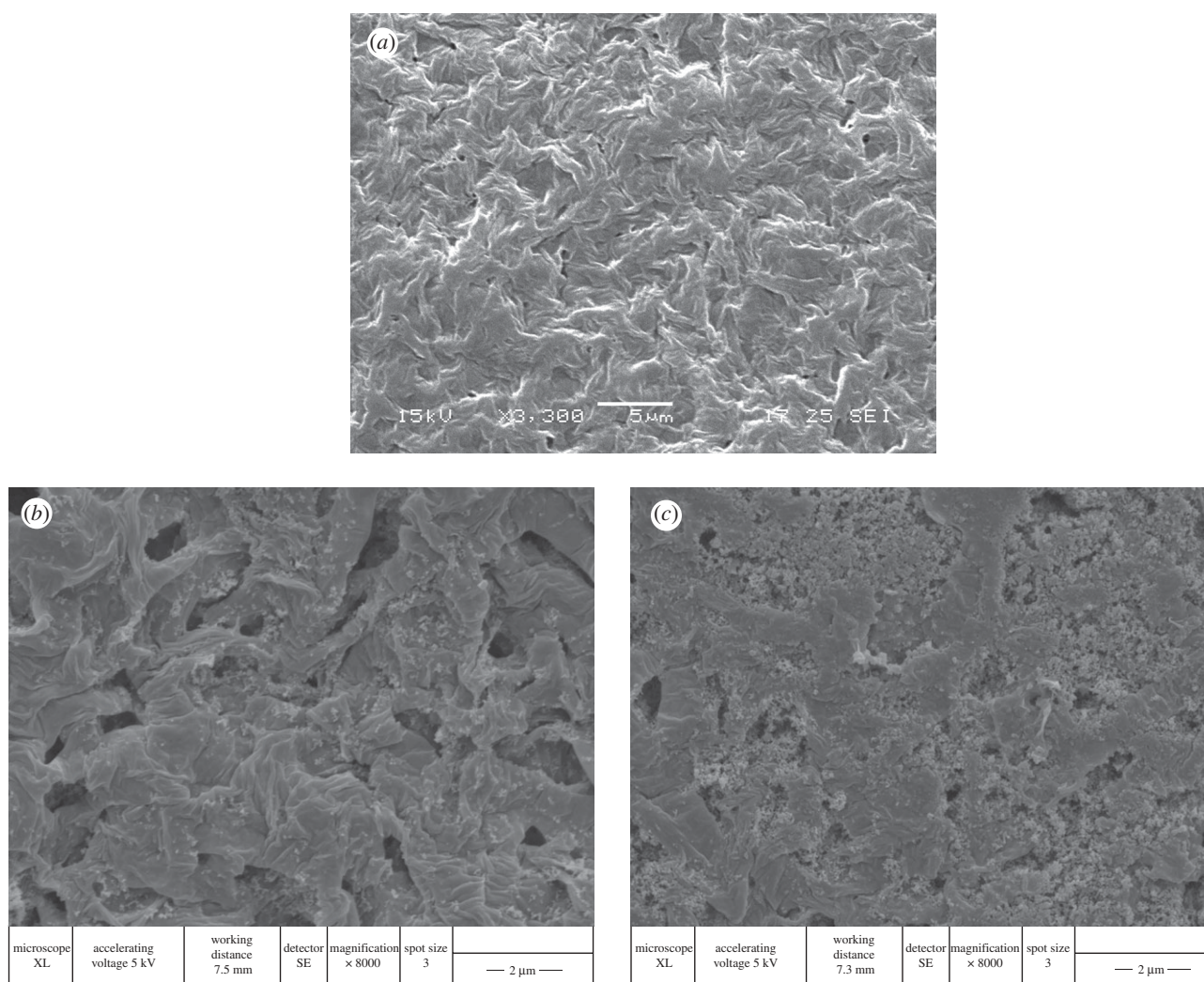


Figure 1. SEM micrographs of (a) P(3HB), (b) P(3HB)/10 wt % n-BG and (c) P(3HB)/20 wt % n-BG.

of the composites is high and, owing to their high surface reactivity, significantly improved the bioactivity of the developed composites, as discussed in subsequent sections. Agglomerations of n-BG particles were also visible on the composite surfaces (e.g. figure 1c). AFM was performed on selected samples to analyse the change in surface roughness induced by the presence of n-BG particles. Key results are presented in figure 2. Figure 2a and d shows the amplitude channel for P(3HB) and P(3HB)/20 wt % n-BG samples, respectively. From the amplitude channel (scan area of $10 \times 10 \mu\text{m}^2$), the morphology of the polymeric film is clearly visible and complementary to the SEM images shown in figure 1. The height channel representations for the polymeric and composite films are shown in figure 2b and e, respectively, and the roughness over an area of $10 \times 10 \mu\text{m}^2$ was measured for all samples. The r.m.s value as indicator of roughness for the entire scanned area was measured to be $186 \pm 2 \text{ nm}$, $220 \pm 10 \text{ nm}$ and $364 \pm 29 \text{ nm}$ for P(3HB), P(3HB)/10 wt % n-BG and P(3HB)/20 wt % n-BG, respectively, quantitatively confirming the SEM observations. Similarly, the average deviations in roughness values are $148 \pm 1 \text{ nm}$, and $292 \pm 25 \text{ nm}$ for P(3HB), P(3HB)/10 wt % n-BG and P(3HB)/20 wt % n-BG, respectively.

3.2. In vitro degradation study

Water uptake (%WA; figure 3a), weight loss (%WL; figure 3b) and change in molecular weight (M_w) of the composites were monitored in this study. Both, the %WA and %WL significantly increased owing to the addition of n-BG particles. The highest water absorption was found to be 32 per cent for the 20 wt % n-BG composites, whereas the neat P(3HB) films had a much lower water uptake (max. 8%), confirming the hydrophobic nature of P(3HB). Similarly, weight loss measurements confirmed that increasing the concentration of n-BG particles increases the weight loss over the studied degradation time. Addition of bioactive glass particles (micron-sized, less than $5 \mu\text{m}$) in the polymeric matrix slowed the molecular weight degradation compared to the P(3HB) on its own (see electronic supplementary material), when immersed in SBF for a period of up to 200 days.

3.3. In vitro bioactivity analysis

Figure 4 shows the SEM micrographs of specimen's surfaces at different time points after immersion in SBF. The nucleation of HA from the nanoscale bioactive glass particles is evident from the SEM micrographs.

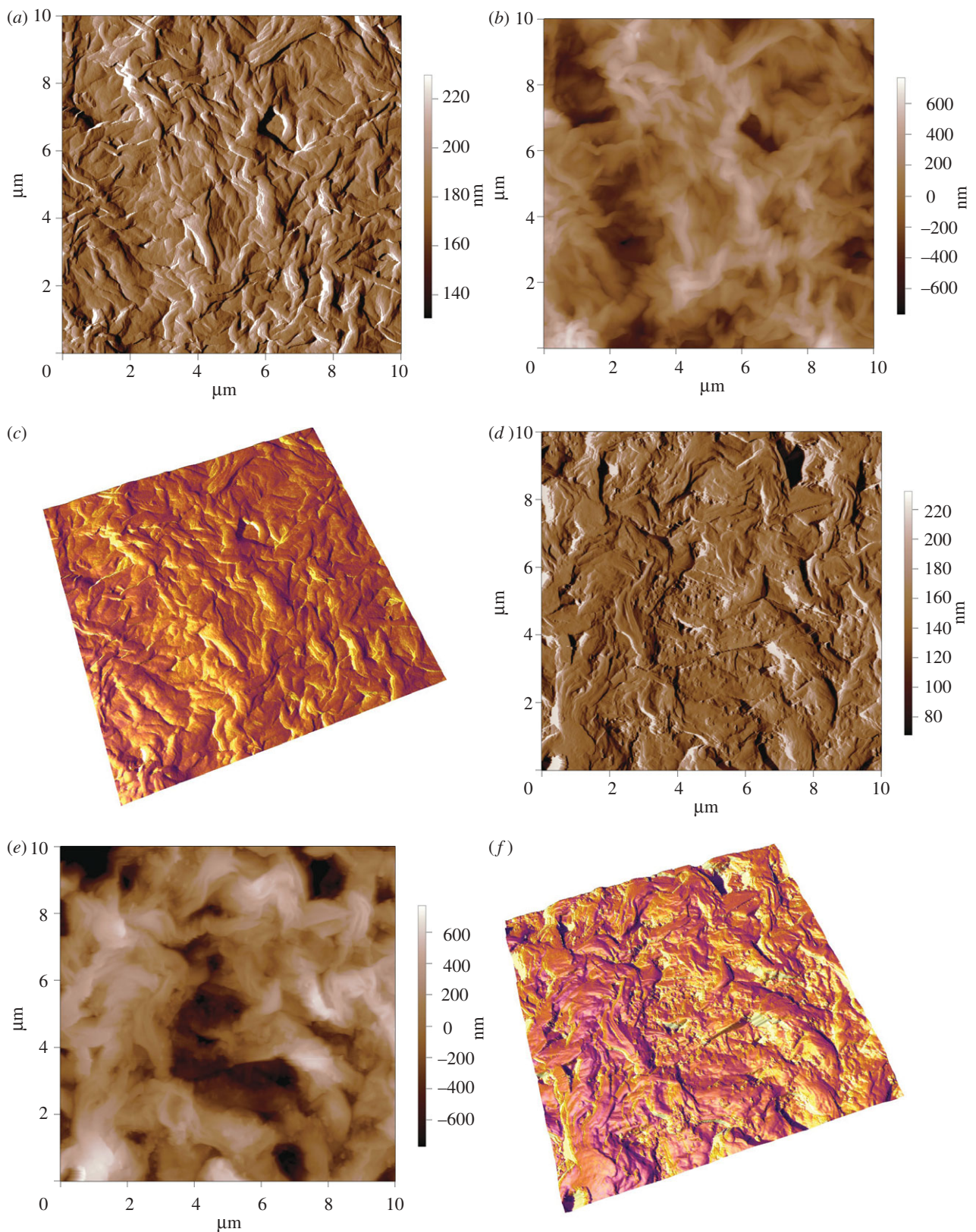


Figure 2. AFM images over a scan area of $10 \times 10 \mu\text{m}^2$ showing the (a) amplitude channel for P(3HB) film, (b) height channel for P(3HB) film, (c) three-dimensional image of P(3HB) film showing the height and the phase channel superimposed, (d) amplitude channel for P(3HB)/20 wt % n-BG film, (e) height channel for P(3HB)/20 wt % n-BG film and (f) three-dimensional image of P(3HB)/20 wt % n-BG film showing the height and the phase channel superimposed.

Figure 4a shows the presence of sub-micron HA nucleating from the n-BG particles, and also shows the homogeneous distribution of HA crystals over the surface. In figure 4e,f, the cross-section images of the

samples confirmed the presence of a uniform layer (thickness $< 10 \mu\text{m}$) of HA on the surface of 10 wt % and 20 wt % n-BG composites after 30 days. The XRD analysis of P(3HB)/n-BG samples (figure 5a) depicts an increase in

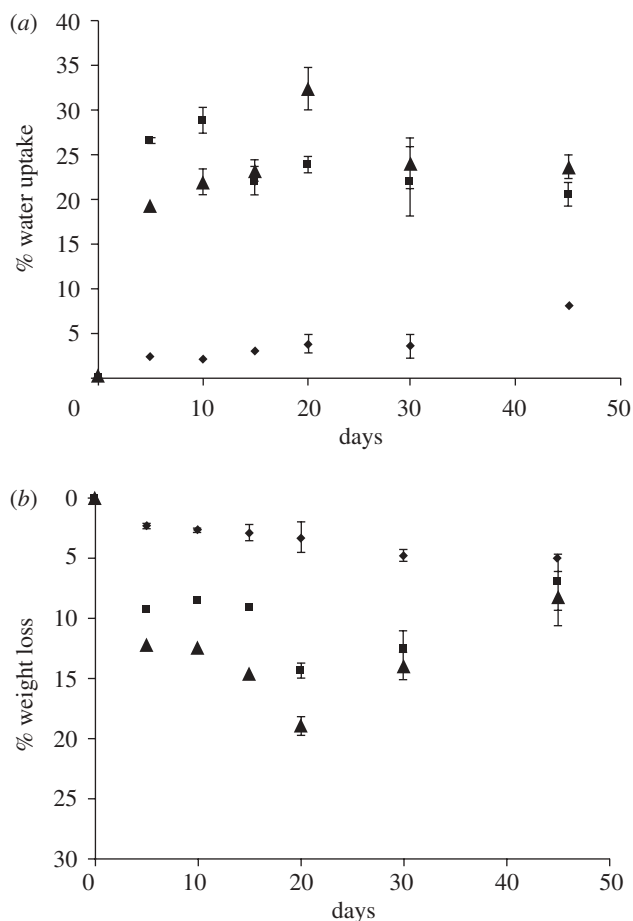


Figure 3. *In vitro* degradation study of P(3HB)/n-BG composites in SBF depicting (a) % water uptake and (b) % weight loss. Diamonds, P(3HB); squares, 10 wt % BG; triangles, 20 wt % BG.

the characteristic crystalline HA peak at 32° (2θ) over the immersion period in SBF. The formation of HA on the samples can be shown to occur from as early as 5 days in SBF, confirming the high bioactivity of the composites owing to the addition of n-BG particles. However, there were no changes observed in the X-ray diffraction pattern and SEM surface morphology for P(3HB) films during the study.

Energy dispersive X-ray (EDX) analysis was conducted to observe the transition of bioactive glass particles to calcium phosphate as well as to detect the nature of the calcium phosphate formed by evaluating the Ca/P ratio for the layer formed on the surfaces upon immersion in SBF. Figure 5b–d shows the transition of bioactive glass particles to calcium phosphate through elemental mapping of Ca, P and Si over the surface of the composite. This change is depicted by the presence of calcium and phosphorus in a given area of the composite and by the depletion of silicon. The EDX results (figure 5e) revealed that the Ca/P ratio on the composite surface gradually increased, stabilizing at 1.58 after 30 days in SBF, indicating a non-stoichiometric HA layer.

The Raman spectroscopic analysis of the composite samples after 5, 10, 30 and 45 days in SBF is shown in figure 6. The HA characteristic (PO_4^{3-}) peak at 964 cm^{-1} was found to increase with increasing

immersion time in SBF. The gradual increase in the PO_4^{3-} peak corresponds to the appearance of crystalline HA layer, which is also documented by the EDX, SEM and XRD results presented above. A typical Raman surface map of the HA layer (intensity distribution of PO_4^{3-} peak at 964 cm^{-1} over a surface area of $70 \times 60\text{ }\mu\text{m}^2$) for the P(3HB)/20 wt % n-BG composite is shown in figure 6b, revealing the distribution of HA on the surface of the composite.

3.4. Cytocompatibility studies

Results of the cytocompatibility study using MG-63 cells on the P(3HB)/n-BG composite surfaces are summarized in figure 7. Figure 7a,b shows cell proliferation to increase in all samples over the 7-day period. The relative cell proliferation data when compared with the control surface (tissue culture plastic) shown in figure 7b indicate that there was no significant difference between the control and the P(3HB) samples at any point during the study period. However, the presence of 20 wt % n-BG in the P(3HB) matrix induced a significant reduction in cell proliferation compared with the control.

ALP activity of the cells was measured for days 7 and 14, as an early marker of osteoblast differentiation (figure 7c). The ALP activity for all samples increased at day 14 with no detectable growth on day 1 (data not shown). The ALP activity was found to be significantly higher in osteogenic growth medium compared with non-osteogenic medium for both time points and for all samples (except for the control). In terms of osteoblastic response to the composite surface as function of n-BG content, it was found that the ALP activity of MG-63 cells was significantly higher than the control surface for days 7 and 14, with 20 wt % n-BG composites exhibiting the highest ALP activity.

The carboxylated-type of osteocalcin (i.e. carboxylated glutamic acid residues (Gla-OC)) produced by the MG-63 osteoblasts when grown on the composite substrates was quantified in this study. On culture day 1, expression of osteocalcin at low levels (average $15 \pm 1\text{ ng}$) was found in all groups (figure 7d), with no significant difference between the composite sample and the control. There was a significant ($*p < 0.05$) difference in the levels of osteocalcin in the osteogenic and non-osteogenic medium for all samples at day 7. A significant ($*p < 0.05$) decrease in osteocalcin levels (in non-osteogenic medium) by adding n-BG particles, compared with the control was also seen on day 7 measurements. On day 14, there was a significant increase in the levels of osteocalcin for all samples (up to 62 and 52% increase on average for osteogenic and non-osteogenic medium, respectively) without having any significant differences between the samples, for both types of medium. At all time points, no significant difference between the control and the P(3HB) samples was observed, thus proving the cytocompatibility of the material.

SEM micrographs of MG-63 cells attached on the surfaces of P(3HB) composites in figure 8 highlight the cell morphology and its attachment to the substrates between days 4 and 7. There were no visible

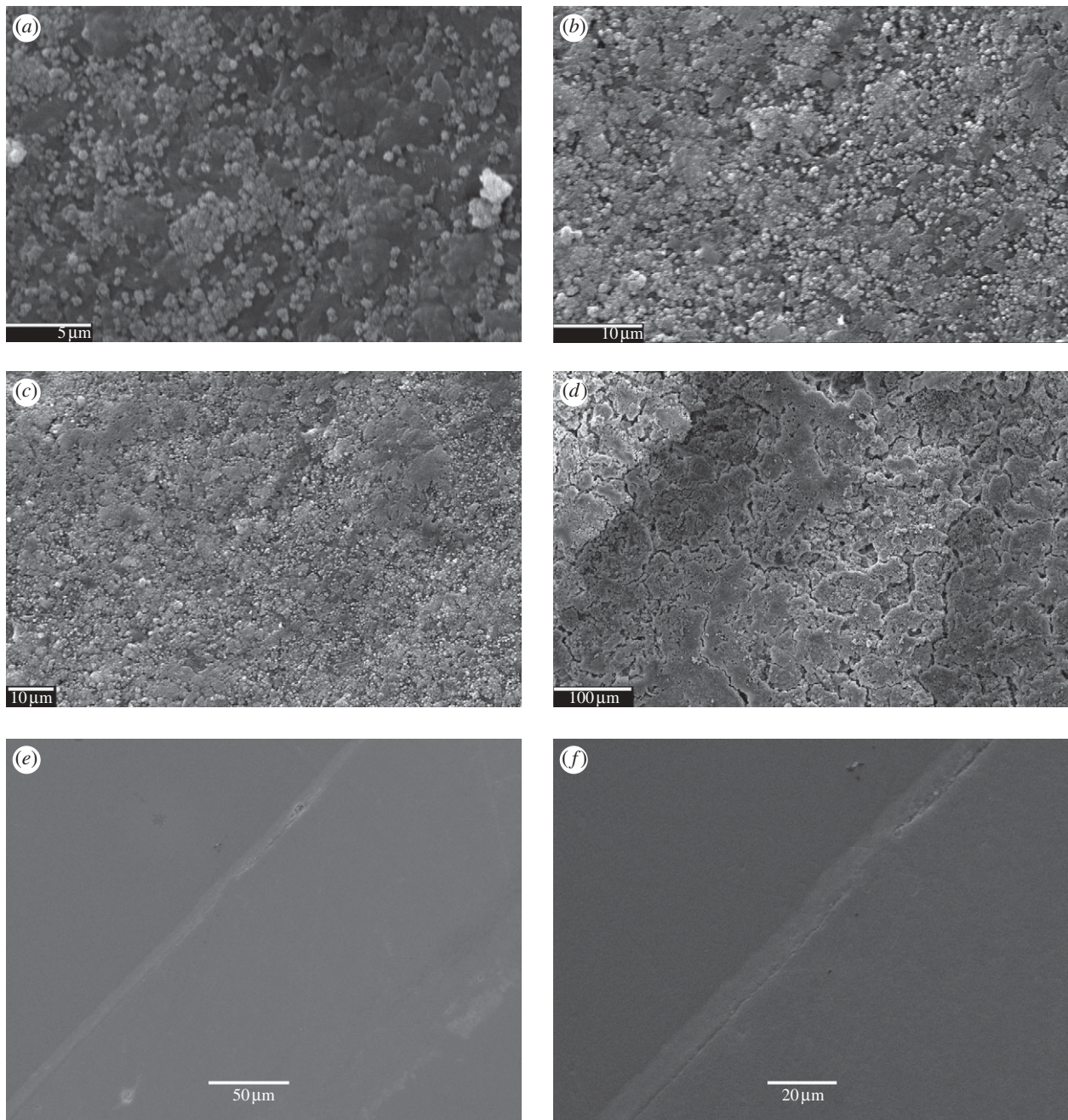


Figure 4. SEM micrographs of P(3HB)/20 wt % n-BG composite samples upon immersion in SBF showing the surface changes owing to the formation of HA layer after (a) 5 days (scale bar, 5 μm), (b) 15 days (scale bar, 10 μm), (c) 30 days (scale bar, 10 μm) and (d) 45 days (scale bar, 100 μm). Cross sections of P(3HB)/n-BG films showing the presence of continuous HA layer after 30 days in SBF for (e) P(3HB)/10 wt % n-BG (scale bar, 50 μm) and (f) P(3HB)/20 wt % n-BG (scale bar, 20 μm).

qualitative differences in the attachment of cells between the neat polymeric and composite samples.

4. DISCUSSION

It has been shown in our earlier work (Misra *et al.* 2008; Schneider *et al.* 2008) that the incorporation of nanoscale fillers in a polymeric matrix enhances the mechanical strength as well as renders conducive surface properties (i.e. better wettability, nanopopography) for biomedical applications. The addition of n-BG particles to the P(3HB) matrix significantly changed the

surface morphology owing to the exposure of the n-BG particles on the surface (figures 1 and 2). The presence of n-BG particles considerably increased the surface roughness of the composites, as determined by both SEM and AFM characterization. The increase of surface roughness plays an important role in cell attachment. This fact in turn had a contributing effect on the bioactivity, water uptake and cytocompatibility of the composite films and stays in line with observations on a similar nanocomposite based on nano tricalcium phosphate in poly(lactide-*co*-glycolic acid) (PLGA; Loher *et al.* 2006). It is important to note that bioactivity studies were not done in the cell culture medium

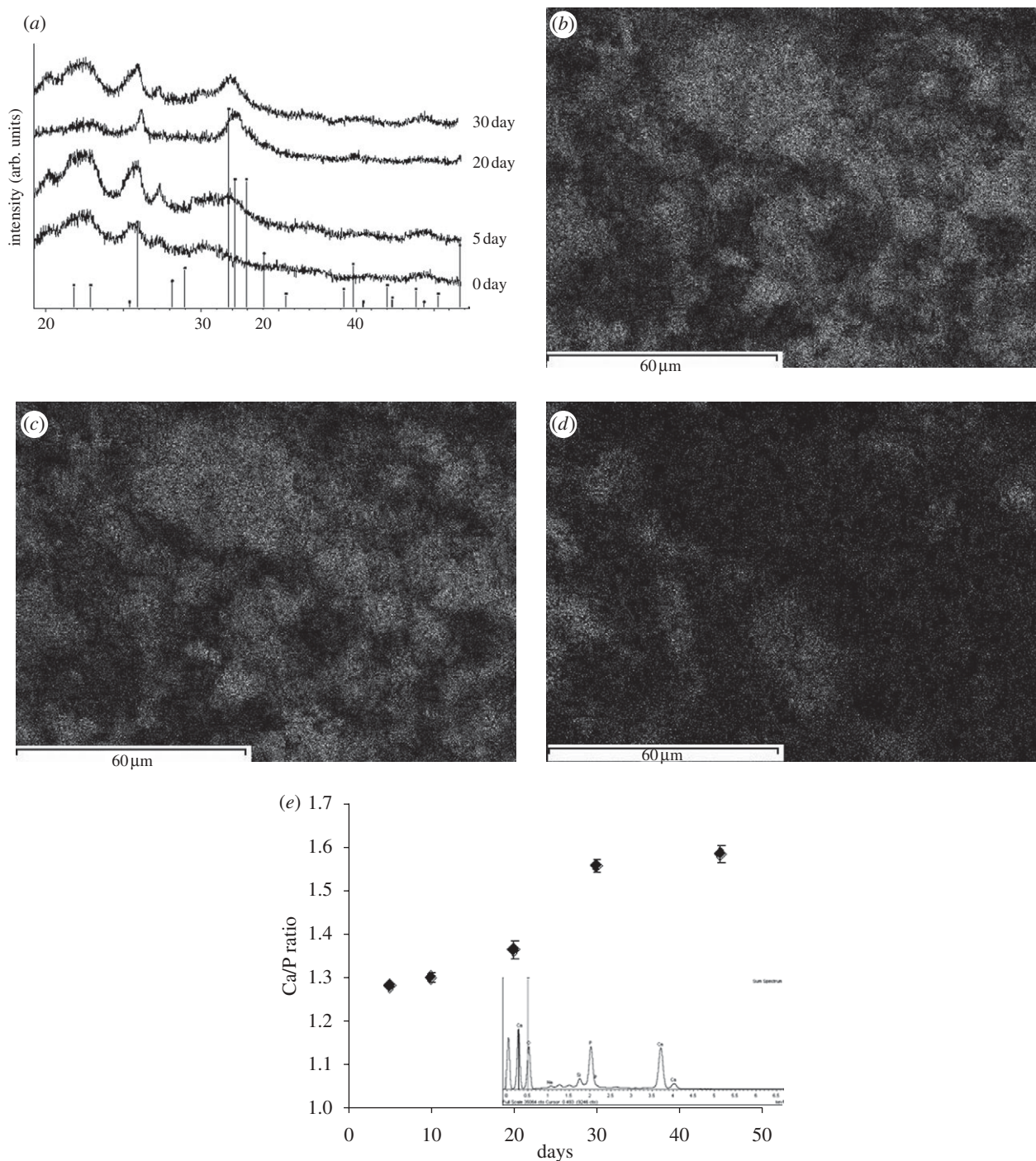


Figure 5. (a) XRD pattern of P(3HB)/n-BG composites highlighting the emergence of crystalline HA peak (denoted by vertical markers) after 5, 20 and 30 days of immersion in SBF. Results of EDX analysis for P(3HB)/20 wt % n-BG composites after 30 days in SBF showing elemental surface mapping of (b) Ca, (c) P, (d) Si, and (e) change in the Ca/P ratio of the HA layer on the composites over the immersion period in SBF.

(DMEM) but they were performed in SBF for a variety of reasons, one of which was that DMEM typically has a calcium content of about 1.82 mM as opposed to SBF at 2.5 mM. This higher Ca content will actively induce the formation of an apatitic bioactive layer on the surfaces, dependent on material surface properties as well as on the reaction of the material with the solution (Hench 1998). Testing of bioactivity of materials intended for bone tissue engineering in SBF is the most extended method in the biomaterials community (Kokubo *et al.* 1990). By testing in solutions of increasing complexity,

i.e. SBF, which contains an ionic composition similar to that of blood plasma and DMEM, which also contains vital organic constituents in the form of proteins, the materials were tested in the appropriate medium according to the parameter under investigation. Thus, biomaterial surfaces are commonly tested in SBF, whereas DMEM is commonly applied where cell studies are considered.

In this context, pre-incubation or passivation of the materials in fully supplemented culture medium is required because of the organic protein content, which

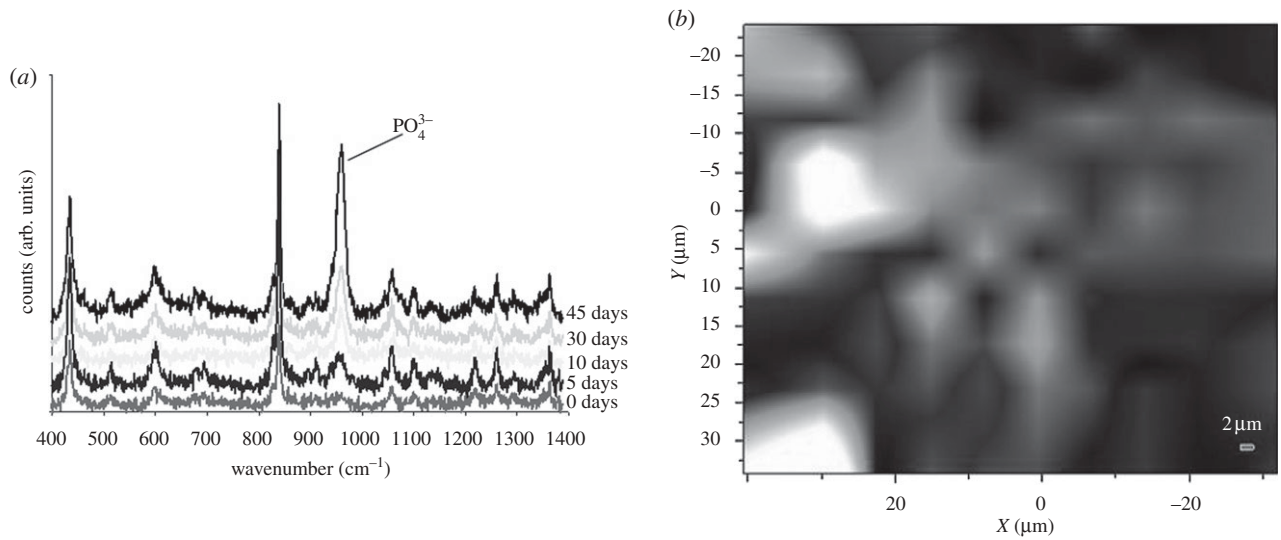


Figure 6. (a) Raman spectra of P(3HB)/20 wt % n-BG composites following 0–45 days immersion in SBF. (b) Raman surface intensity map of PO_4^{3-} peak at 964 cm^{-1} for P(3HB)/20 wt % n-BG composites after 45 days of SBF immersion. The bright areas denote high intensities, whereas black areas denote low intensity of the PO_4^{3-} peak. Raman map for 0 days not shown as there is no presence of PO_4^{3-} peak.

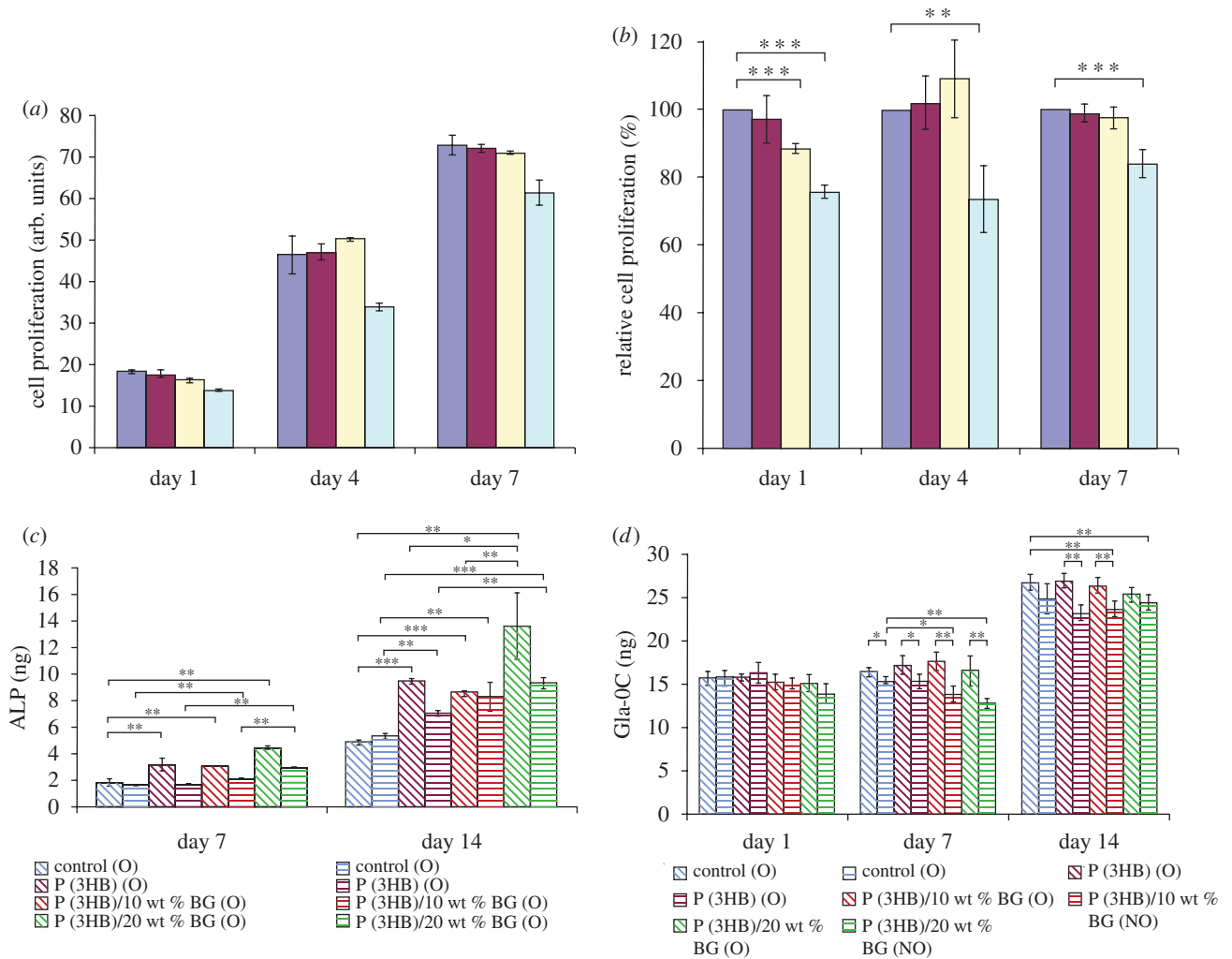


Figure 7. Cytocompatibility studies of P(3HB)/n-BG composites using MG-63 osteoblasts showing (a) cell proliferation measurements for 1, 4 and 7 days, using AB assay, (b) cell proliferation of all tested samples relative to the control (control set to 100%), (c) ALP activity for osteoblastic phenotype expression of MG-63 cells grown on P(3HB)/n-BG samples using osteogenic (O) and non-osteogenic (NO) medium. (d) Osteocalcin content of culture medium (osteogenic (O) and non-osteogenic (NO) medium) as a function of time. Measurements correspond to osteocalcin levels on days 7 and 14 ($n = 3$, error bars = \pm s.d.; $*p < 0.05$, $**p < 0.01$, $***p < 0.001$). (a) and (b) Violet, control; maroon, P(3HB); yellow, 10 per cent n-BG; light blue, 20 per cent n-BG.

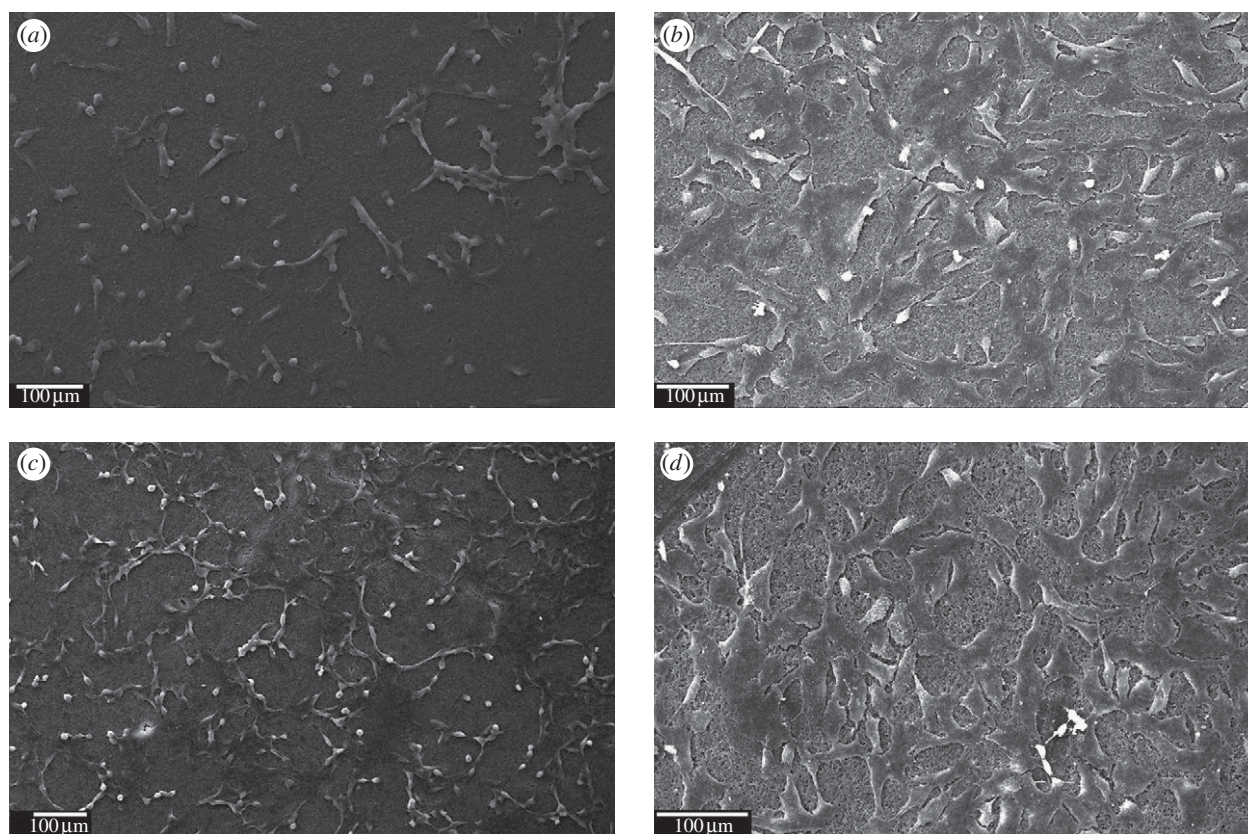


Figure 8. SEM images showing MG-63 cells grown on (a) P(3HB) at day 4, (b) P(3HB) at day 7, (c) P(3HB)/20 wt % n-BG at day 4, and (d) P(3HB)/20 wt % n-BG at day 7. Scale bar, 100 μm .

is lacking in SBF, which only consists of inorganic products. The importance of a modified protein layer upon a material surface is well recognized, which will help cells attach, spread, proliferate and differentiate upon the material, regardless of its original composition and any subsequent precipitation of inorganic apatite layers. The presence of proteins is essential to allow adequate cell attachment and valid *in vitro* cell assays to be performed. Indeed, a biomimetic apatite layer is also produced in DMEM containing serum, but is not as mature as that formed in SBF alone under the same conditions (Faure *et al.* 2009).

The %WL and %WA measurements of the composites after immersion in SBF were shown to increase on increasing the n-BG particle concentration. The observation also confirmed the hydrophobic nature of the polymer and its slow degradation over time (Freier *et al.* 2002). The increase in water uptake can be attributed to the increase in the hydrophilicity of the composites owing to the addition of n-BG (Misra *et al.* 2008), whereas the increased weight loss could be related to the dissolution of the n-BG particles, as previously reported for other composites (Loher *et al.* 2006; Li & Chang 2005a). The temporal variation in the weight average (M_w) and number average (M_n) molecular weight of the P(3HB)/bioactive glass (micron-sized particles) highlights the continuous drop in M_w without the characteristic induction period described by Doi *et al.* (1989) for the P(3HB) samples (see electronic supplementary material). The overall change in M_w for the composites followed first-order

kinetics, with a half-life of 18 weeks. Although the size of the bioactive glass particles used for the M_w measurements was less than 5 μm , it provided valuable information about the buffering effect induced by the release of alkaline ions from the inorganic particles preventing the accelerated degradation because of the acidification of the medium owing to acidic products of the P(3HB) degradation (Gopferich 1996).

The release of ions (PO_4^{3-} , Na^+ and Ca^{2+}) upon immersion of P(3HB)/n-BG composites in water was also examined using ion chromatography over the 45-day period and it was observed that the ion release was higher for 20 wt % n-BG composites than for 10 wt % n-BG composites. The graphs also show the classical two stage release with sodium being released rapidly and at early time points followed by a slower release of other ions (see electronic supplementary material).

The bioactivity of P(3HB)/n-BG composites was demonstrated in this investigation by monitoring the three different aspects, i.e. morphology (SEM), crystallinity (XRD) and chemistry (Raman spectroscopy and EDX). The bioactivity of the composites, determined by the formation of HA on the surface upon immersion in SBF, was confirmed within 5 days (figure 4a). The presence of a uniform layer (less than 10 μm) of HA on the surface was observed after 30 days, as shown in figure 4e,f. Formation of HA was also confirmed using XRD (figure 5a), wherein the intensity of the prominent crystalline peak from HA at ($2\theta = 31^\circ - 32^\circ$) increased by prolonging the immersion time. The

calcium–phosphorus ratio (Ca/P) of the HA layer was evaluated at different time intervals using EDX. The Ca/P ratio increased to 1.58 after 30 days of immersion in SBF, which is lower than the Ca/P ratio of stoichiometric HA, i.e. 1.67. An elemental surface mapping for silicon, calcium and phosphorus in a fixed area highlighted the transition of bioactive glass to calcium phosphate (figure 5). Raman micro-spectroscopy has been shown to be sensitive towards the detection of HA (Clupper *et al.* 2004). The peak at 964 cm^{-1} (figure 6*a*) corresponds to the P–O symmetric stretching vibrations in PO_4^{3-} groups in HA. This peak was found to increase with time (figure 6), which indicates the growth of the HA layer on the composite's surface. Raman spectroscopy analysis can be used as a convenient tool to monitor the bioactivity of samples *in situ* owing to the insensitivity of Raman spectra to the presence of water. The intensity map of wavelength 964 cm^{-1} confirms a strong degree of HA formation over the surface of the composite and hence further confirms high degree of bioactivity for the P(3HB)/n-BG composites. The high formation rate of HA layer on the P(3HB)/n-BG composites upon immersion in SBF is thought to be influenced by the high water-uptake capacity of the matrix, which further favours the dissolution of the bioactive glass nanoparticles.

Cell proliferation studies (cells grown on non-osteogenic medium), indicated the suitability of all the samples to allow for cell proliferation (figure 7*a,b*). In contrast to the addition of 10 wt % n-BG, addition of 20 wt % n-BG particles significantly reduced the proliferation of cells compared with the control (not less than 65% of the control) on days 1, 4 and 7. ALP activity and osteocalcin levels were further measured over a 14-day period to evaluate osteoblast activation and differentiation, as these monitors (ALP and osteocalcin) are the typical markers for osteoblast characterization (Cowles *et al.* 1998; Malaval *et al.* 1999). In terms of osteoblastic response to the composite surface as a function of n-BG content, it was found that the ALP activity of MG-63 cells in the P(3HB)/n-BG group was significantly higher than the control surface for days 7 and 14, with the presence of 20 wt % n-BG causing the highest increase (figure 7*c*). The addition of n-BG particles induced topographical features (change in roughness) on the surface that might help the anchorage and attachment of the cells to the surface. The increase in ALP activity was also significantly higher for cells grown in osteogenic medium than for cells grown in non-osteogenic medium and was also higher for cells grown on the P(3HB)/n-BG groups indicating the materials alone may have initiated a greater production/expression of osteocalcin by the cells. Multiple studies have suggested that ALP activity is enhanced when osteoblasts are grown on bioactive glass substrates (Loty *et al.* 2001; Bosetti & Cannas 2005). A possible reason for the increased bone formation around bioactive glass implants is either the enhanced attachment of bone to the bioactive glass owing to the high surface reactivity of the glass or owing to exposure to the glass dissolution products, which enhances osteoblastic differentiation that affects cell gene expression (Xynos *et al.* 2001;

Bosetti & Cannas 2005). Similar results using mesenchymal stem cells have reported higher ALP activity for PLGA/BG foams in comparison to PLGA foams (Reilly *et al.* 2007). Yang *et al.* (2006) also showed that poly(DL-lactic acid) (PDLLA) foams containing 5 wt % BG (micron-sized) were much more effective in increasing ALP activity than 40 wt % BG/PDLLA foams.

Osteocalcin constitutes about 15 per cent of the non-collagenous bone matrix proteins and is produced exclusively in osteoblasts and odontoblasts (Price 1989). It is suggested that when there is increased bone formation, the serum osteocalcin concentration also increases (Deftos *et al.* 1982). In this study, osteocalcin production was higher for samples incubated in osteogenic medium compared with non-osteogenic medium, with the level of osteocalcin for all the samples being significantly higher on day 14 (figure 7*d*). There was no significant change (compared with the control) in the osteocalcin production owing to the addition of n-BG particles. In a similar study, Schneider *et al.* (2008) did not find significantly different *in vitro* osteocalcin levels when comparing PLGA and composites containing up to 40 wt % tricalcium phosphate nanoparticles while using osteogenic medium. However, there was a significant decrease in osteocalcin production on day 7 for the P(3HB)/n-BG samples compared with the control surface, when incubated in a non-osteogenic medium. Similar levels of osteocalcin were also produced by mouse osteoblast cell lines when grown on collagen foams (Arpornmaeklong *et al.* 2007) and on P(3HB-co-3HV) substrates (Kose *et al.* 2003). The increase in osteocalcin as observed in figure 7*d* is indicative of the maturation of the cells and their osteoblastic phenotype and also complements the increase of ALP activity of MG-63 cells on day 14. Finally, the ALP and the osteocalcin measurements suggest that the osteogenic medium facilitated a better growth and differentiation medium than the non-osteogenic medium for MG-63 osteoblasts. *In vivo* studies (subcutaneous implants in rats) were also conducted on the newly isolated P(3HB) showing a non-toxic and a foreign body response (see electronic supplementary material). Further experiments involving three-dimensional P(3HB)/BG foams (scaffolds) are presently being conducted to ascertain the *in vivo* response of the composite structures.

5. CONCLUSIONS

The main conclusions from this experimental study can be summarized as follows.

- (i) Addition of n-BG particles to P(3HB) significantly changes the surface morphology of the composites, which further enhanced the %WA, bioactivity, and %WL.
- (ii) The bioactive HA layer formation in contact with SBF was found to be uniformly distributed over the entire surface on the P(3HB)/n-BG composites at an early stage of immersion and was shown to grow (less than $10\text{ }\mu\text{m}$ thickness) over the period of 45 days.

- (iii) Cytocompatibility study of P(3HB)/n-BG composites highlighted the ability of the MG-63 cells to attach, proliferate and differentiate on all substrates. In most cases, the results were similar to the control surface and further strengthened the use of the composites as a suitable material to develop scaffolds for hard tissue applications.

The authors gratefully acknowledge the financial help of Overseas Research Scholarship, IDEA League Research Grant and Gebert Rűf Foundation GRS 048/04. Assistance from Xin Zhao and Dr Graham Palmer (Eastman Dental Institute, UCL, London) was instrumental in conducting the Raman spectroscopy measurements. Support of Dr Thurecht Kristofer (University of Nottingham) for molecular weight analysis is greatly appreciated. The assistance of Mr Nick Royall (Imperial College, London) for EDX analysis is also acknowledged. The authors are very grateful to the referees for their valuable and informative comments and we feel the edits to the manuscript as a result of their suggestions has added greatly to the scientific value of our paper.

REFERENCES

- Arpornmaeklong, P., Suwatwirote, N., Pripatnanot, P. & Oungbho, K. 2007 Growth and differentiation of mouse osteoblasts on chitosan–collagen sponges. *Int. J. Oral Maxillofac. Surg.* **36**, 328–337. (doi:10.1016/j.ijom.2006.09.023)
- Barrere, F., Mahmood, T. A., de Groot, K. & van Blitterswijk, C. A. 2008 Advanced biomaterials for skeletal tissue regeneration: instructive and smart functions. *Mater. Sci. Eng. R* **59**, 38–71. (doi:10.1016/j.mser.2007.12.001)
- Blaker, J. J., Gough, J. E., Maquet, V., Notingher, I. & Boccaccini, A. R. 2003 *In vitro* evaluation of novel bioactive composite based on Bioglass filled polylactide foams for bone tissue engineering scaffolds. *J. Biomed. Mater. Res. Part A* **67**, 1401–1411. (doi:10.1002/jbm.a.20055)
- Bosetti, M. & Cannas, M. 2005 The effect of bioactive glasses on bone marrow stromal cells differentiation. *Biomaterials* **26**, 3873–3879. (doi:10.1016/j.biomaterials.2004.09.059)
- Brunner, T. J., Grass, R. N. & Stark, W. J. 2006 Glass and bioglass nanopowders by flame synthesis. *Chem. Commun.* **13**, 1384–1386. (doi:10.1039/b517501a)
- Chen, G. Q. & Wu, Q. 2005 The application of polyhydroxyalkanoate as tissue engineering materials. *Biomaterials* **26**, 6565–6578. (doi:10.1016/j.biomaterials.2005.04.036)
- Clupper, D. C., Gough, J. E., Embanga, P. M., Notingher, I., Hench, L. L. & Hall, M. M. 2004 Bioactive evaluation of 45S5 bioactive glass fibers and preliminary study of human osteoblast attachment. *J. Mater. Sci. Mater. Med.* **15**, 803–808. (doi:10.1023/B:JMSM.0000032821.32577.fc)
- Couto, D. S., Hong, Z. & Mano, J. F. 2009 Development of bioactive and biodegradable chitosan-based injectable systems containing bioactive glass nanoparticles. *Acta Biomater.* **5**, 115–123. (doi:10.1016/j.actbio.2008.08.006)
- Cowles, E. A., DeRome, M. E., Pastizzo, G., Brailey, L. L. & Gonowicz, G. A. 1998 Mineralization and the expression of matrix proteins during *in vivo* bone development. *Calcif. Tissue Int.* **62**, 74–82. (doi:10.1007/s002239900397)
- Deftos, L. J., Parthemore, J. G. & Price, P. A. 1982 Changes in plasma bone GLA protein during treatment of bone disease. *Calcif. Tissue Int.* **34**, 121–124. (doi:10.1007/BF02411221)
- Doi, Y., Kaneshawa, Y., Kawaguchi, Y. & Kunioka, M. 1989 Hydrolytic degradation of microbial poly(hydroxyalkanoates). *Makrom. Chem. Rapid. Commun.* **10**, 227–230. (doi:10.1002/marc.1989.030100506)
- Faure, J., Balamurugan, A., Benhayoune, H., Torres, P., Balossier, G. & Ferreira, J. M. F. 2009 Morphological and chemical characterisation of biomimetic bone like apatite formation on alkali treated Ti6Al4V titanium alloy. *Mater. Sci. Eng. C* **29**, 1252–1257. (doi:10.1016/j.msec.2008.09.047)
- Freier, T., Kunze, C., Nischan, C., Kramer, S., Sternberg, K., Sab, M., Hopt, U. T. & Schmitz, K. P. 2002 *In vitro* and *in vivo* degradation studies for development of a biodegradable patch based on poly(3-hydroxybutyrate). *Biomaterials* **23**, 2649–2657. (doi:10.1016/S0142-9612(01)00405-7)
- Gopferich, A. 1996 Mechanisms of polymer degradation and erosion. *Biomaterials* **17**, 103–114. (doi:10.1016/0142-9612(96)85755-3)
- Guarino, V., Causa, F. & Ambrosio, L. 2007 Bioactive scaffolds for bone and ligament tissue. *Exp. Rev. Med. Devices* **4**, 405–418. (doi:10.1586/17434440.4.3.405)
- Helen, W. & Gough, J. E. 2006 *In vitro* studies of annulus fibrosus disc cell attachment, differentiation and matrix production on PDLA/45S5 Bioglass composite films. *Biomaterials* **27**, 5220–5229. (doi:10.1016/j.biomaterials.2006.06.008)
- Hench, L. L. 1998 Biomaterials: a forecast for the future. *Biomaterials* **19**, 1419–1423. (doi:10.1016/S0142-9612(98)00133-1)
- Knowles, J. C. & Hastings, G. W. 1992 *In vitro* degradation of polyhydroxybutyrate/polyhydroxyvalerate copolymer. *J. Mater. Sci. Mater. Med.* **3**, 352–358. (doi:10.1007/BF00705367)
- Kokubo, T., Kushitani, H., Sakka, S., Kitsugi, T. & Yamamuro, T. 1990 Solutions able to reproduce *in vivo* surface structure changes in bioactive glass ceramic A-W. *J. Biomed. Mater. Res.* **24**, 721–734. (doi:10.1002/jbm.820240607)
- Kose, G. T., Korkusuz, F., Korkusuz, P., Purali, N., Ozkul, A. & Hasirci, V. 2003 Bone generation on PHBV matrices: an *in vitro* study. *Biomaterials* **24**, 4999–5007. (doi:10.1016/S0142-9612(03)00417-4)
- Li, H. & Chang, J. 2005a *In vitro* degradation of porous degradable and bioactive PHBV/Wollastonite composite scaffolds. *Polym. Degrad. Stabil.* **87**, 301–307. (doi:10.1016/j.polymdegradstab.2004.09.001)
- Li, H. & Chang, J. 2005b pH-compensation effect of bioactive inorganic fillers on the degradation of PLGA. *Compos. Sci. Technol.* **65**, 2226–2232. (doi:10.1016/j.compscitech.2005.04.051)
- Liu, A., Hong, Z., Zhuang, X., Chen, X., Cui, Y., Liu, Y. & Jing, X. 2008 Surface modification of bioactive glass nanoparticles and the mechanical and biological properties of poly(L-lactide) composites. *Acta Biomater.* **4**, 1005–1015. (doi:10.1016/j.actbio.2008.02.013)
- Loher, S., Reboul, V., Brunner, T. J., Simonet, M., Dora, C., Neuenschwander, P. & Stark, W. J. 2006 Improved degradation and bioactivity of amorphous aerosol derived tricalcium phosphate nanoparticles in poly(lactide-co-glycolide). *Nanotechnology* **17**, 2054–2061. (doi:10.1088/0957-4484/17/8/044)
- Loty, C. *et al.* 2001 Bioactive glass stimulates *in vitro* osteoblast differentiation and creates a favorable template for bone tissue formation. *J. Bone Miner. Res.* **16**, 231–239. (doi:10.1359/jbmr.2001.16.2.231)

- Luklinska, Z. B. & Bonfield, W. 1997 Morphology and ultrastructure of the interface between hydroxyapatite-polyhydroxybutyrate composite implant bone. *J. Mater. Sci. Mater. Med.* **8**, 379–383. (doi:10.1023/A:1018589018205)
- Malaval, L., Liu, F., Roche, P. & Aubin, J. E. 1999 Kinetics of osteoprogenitor proliferation and osteoblast differentiation *in vitro*. *J. Cell. Biochem.* **74**, 616–627. (doi:10.1002/(SICI)1097-4644(19990915)74:4<616::AID-JCB11>3.0.CO;2-Q)
- Misra, S. K., Valappil, S. P., Roy, I. & Boccaccini, A. R. 2006 Polyhydroxyalkanoate (PHA)/inorganic phase composites for tissue engineering applications. *Biomacromolecules* **7**, 2249–2258. (doi:10.1021/bm060317c)
- Misra, S. K., Mohn, D., Brunner, T. J., Stark, W. J., Philip, S. E., Roy, I., Salih, V., Knowles, J. C. & Boccaccini, A. R. 2008 Comparison of nanoscale and microscale bioactive glass on the properties of P(3HB)/Bioglass composites. *Biomaterials* **29**, 1750–1761. (doi:10.1016/j.biomaterials.2007.12.040)
- Price, P. A. 1989 Gla containing proteins of bone. *Connect. Tissue Res.* **21**, 51–57. (doi:10.3109/03008208909049995)
- Reilly, G. C., Radin, S., Chen, A. T. & Ducheyne, P. 2007 Differential alkaline phosphatase response of rat and human bone marrow derived mesenchymal stem cells to 45S5 bioactive glass. *Biomaterials* **28**, 4091–4097. (doi:10.1016/j.biomaterials.2007.05.038)
- Rezwan, K., Chen, Q. Z., Blaker, J. J. & Boccaccini, A. R. 2006 Biodegradable and bioactive porous polymer/inorganic composite scaffolds for bone tissue engineering. *Biomaterials* **27**, 3413–3431. (doi:10.1016/j.biomaterials.2006.01.039)
- Schneider, O. D., Loher, S., Brunner, T. J., Uebersax, L., Simonet, M., Grass, R. N., Merkle, H. P. & Stark, W. J. 2008 Cotton wool like nanocomposite biomaterials: *in vitro* bioactivity and osteogenic differentiation of human mesenchymal stem cells. *J. Biomed. Mater. Res. Part B* **84**, 350–362.
- Valappil, S. P., Misra, S. K., Boccaccini, A. R., Keshvaraz, T., Bucke, C. & Roy, I. 2007 Large scale production and efficient recovery of PHB with desirable material properties, from the newly characterised *Bacillus cereus* SPV. *J. Biotechnol.* **132**, 251–258. (doi:10.1016/j.jbiotec.2007.03.013)
- Waltimo, T., Brunner, T. J., Vollenweider, M., Stark, W. J. & Zehnder, M. 2007 Antimicrobial effect of nanometric bioactive glass 45S5. *J. Dental Res.* **86**, 754–757. (doi:10.1177/154405910708600813)
- Wang, Y. W., Wu, Q., Chen, J. & Chen, G. Q. 2005 Evaluation of three-dimensional scaffolds made of blends of hydroxyapatite and poly(3-hydroxybutyrate-co-3-hydroxyhexanoate) for bone reconstruction. *Biomaterials* **26**, 899–904. (doi:10.1016/j.biomaterials.2004.03.035)
- Williams, S. F. & Martin, D. P. 2002 Applications of PHAs in medicine and pharmacy. In *Biopolymers: polyesters III*, vol. 4 (eds Y. Doi & A. Steinbüchel), p. 91. Weinheim, Germany: Wiley.
- Xiao, X. Q., Zhao, Y. & Chen, G. Q. 2007 The effect of 3-hydroxybutyrate and its derivatives on the growth of glial cells. *Biomaterials* **28**, 3608–3616. (doi:10.1016/j.biomaterials.2007.04.046)
- Xynos, I. D., Edgar, A. J., Buttery, L. D. K., Hench, L. L. & Polak, J. M. 2001 Gene expression profiling of human osteoblasts following treatment with the ionic products of Bioglass 45S5 dissolution. *J. Biomed. Mater. Res.* **55**, 151. (doi:10.1002/1097-4636(200105)55:2<151::AID-JBM1001>3.0.CO;2-D)
- Yang, X. B., Webb, D., Blaker, J. J., Boccaccini, A. R., Maquet, V., Cooper, C. & Oreffo, R. O. C. 2006 Evaluation of human bone marrow stromal cell growth on biodegradable polymer/Bioglass composites. *Biochem. Biophys. Res. Commun.* **342**, 1098–1107. (doi:10.1016/j.bbrc.2006.02.021)